Switching Exciton Pulses Through Conical Intersections

K. Leonhardt,* S. Wüster, and J. M. Rost
Max Planck Institute for the Physics of Complex Systems, Nöthnitzer Strasse 38, 01187 Dresden, Germany
(Received 25 October 2013; published 24 November 2014)

Exciton pulses transport excitation and entanglement adiabatically through Rydberg aggregates, assemblies of highly excited light atoms, which are set into directed motion by resonant dipole-dipole interaction. Here, we demonstrate the coherent splitting of such pulses as well as the spatial segregation of electronic excitation and atomic motion. Both mechanisms exploit local nonadiabatic effects at a conical intersection, turning them from a decoherence source into an asset. The intersection provides a sensitive knob controlling the propagation direction and coherence properties of exciton pulses. The fundamental ideas discussed here have general implications for excitons on a dynamic network.

DOI: 10.1103/PhysRevLett.113.223001 PACS numbers: 32.80.Ee, 31.50.Gh, 34.20.Cf, 82.20.Rp

Introduction.—Frenckel excitons [1], in which excitation energy of an interacting quantum system is coherently shared among several constituents, are a fundamental ingredient of photosynthetic light harvesting [2]. Recently, they have become accessible in ultracold Rydberg gases, due to strong long-range dipole-dipole interactions [3–11] and large lifetimes of atomic Rydberg states [12,13]. Assemblies of several regularly placed and Rydberg excited cold atoms—flexible Rydberg aggregates—provide new concepts such as adiabatic guiding of an exciton through atomic chains as an exciton pulse [14–16]. Such a pulse is initiated by a displacement of one atom in the regular chain. The displacement simultaneously localizes the exciton on the atom pair with the smallest separation and initiates the pulse, i.e., the motion of the exciton. Subsequent binary collisions propagate the exciton pulse and the associated entanglement through the chain with very high fidelity. Without atomic motion, this would require careful tuning of interactions [17–20].

That this propagation along a one-dimensional (1D) chain of atoms preserves the exciton with high fidelity [15] is remarkable, since the transport appears quite fragile requiring a lossless locking in of electronic excitation transfer and atomic motion. However, exciton transport often occurs in higher dimensional systems, where it is *a priori* unclear if we can also guide and control the exciton pulse. Already, a two-dimensional setup of atoms gives rise to conical intersections (CIs) [21] which might compromise adiabaticity known to be an important prerequisite of exciton transport. On the other hand, CIs can play constructive roles in photochemical processes [22], and hence, might be similarly useful for atomic aggregates.

In the following, we will show how an exciton pulse can be coherently split through a CI that arises between two excitonic Born-Oppenheimer (BO) surfaces of the system. The junction between two atomic chains that gives rise to the conical intersection can be functionalized in two ways, as a beam splitter or a switch, sending the pulse split in both directions on the second chain or in only the one preselected. The surfaces involved in the CI serve as output modes of the beam splitter. We will explicitly demonstrate that the junction constitutes a sensitive point where essential characteristics of the exciton pulse propagation can be controlled through small shifts in external trapping parameters. Our results concern exciton transport on any network whose constituents move, such as (artificial) light-harvesting devices [19].

T-shaped aggregates.—The junction is created with two chains of Rydberg atoms in a T shape configuration [Fig. 1(a)], with the required one-dimensional confinement generated optically [23,24]. Specifically, we will use $2N$ Rydberg atoms with mass $M = 11\,000$ a.u. and principal quantum number $\nu = 44$. We assume that N of these atoms are constrained on the x axis, and the other N on the y axis, such that all atoms can only move freely in one dimension. We start with one Rydberg atom in an angular momentum p state, while the rest are in s states. The electronic wave function $|\psi_{\rm el}(\mathbf{R})\rangle$ of the whole system can be expanded in the single excitation basis $|\psi_{\rm el}(\mathbf{R})\rangle = \sum_{n=1}^{2N} c_n(t)|\pi_n\rangle$, where $|\pi_n\rangle = |s, \ldots, p, \ldots, s\rangle$ is the state with the nth atom in the p state [14–16] and $\mathbf{R} = (\mathbf{R}_1, \ldots, \mathbf{R}_{2N})^{\rm T}$ groups all atomic coordinates $\mathbf{R}_n$. The system is ruled by the Hamiltonian

$$\hat{H} = -\frac{\hbar^2}{2M}\nabla^2_{\mathbf{R}} + \sum_{m\neq n=1}^{2N} (\hat{V}_{\rm dd}(R_{mn}) + \hat{V}_{\rm VDW}(R_{mn})), \qquad (1)$$

where $R_{mn} = |\mathbf{R}_m - \mathbf{R}_n|$ is the distance between atoms m and n.

The long-range Rydberg-Rydberg interactions [12] are described with two explicit contributions $\hat{V}_{\rm dd}$ and $\hat{V}_{\rm VDW}$, a resonant dipole-dipole (dd) and a van der Waals (VDW) term, respectively. $\hat{V}_{\rm dd}$ couples excitations $|\pi_n\rangle$ on different atoms n through

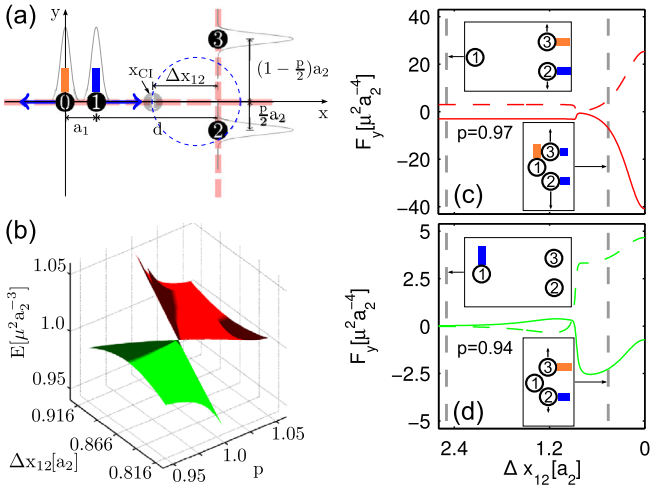

FIG. 1 (color online). (a) Orthogonal atom chains with one Rydberg dimer each. Atoms 0 and 1 initially share an excitation, due to which atom 1 reaches the conical intersection at x_{CI}. The origin of the coordinate system is set to the mean initial position of atom 0. (b) The repulsive energy surface U_{rep} (red) and middle surface U_{mid} (green) of the trimer subunit (atoms 1, 2, and 3) near the CI. (c),(d) Forces on atom 2 (solid lines) and atom 3 (dashed lines), for the repulsive surface [red, (c)] and middle surface [green, (d)]. The insets show atomic positions and the excitation distribution (d_n, see text) of exciton states and forces for the indicated values of Δx_{12}, which denotes the distance between atom 1 and the vertical chain. The parameter p controls the degree of symmetry of the trimer, where $p = 1$ corresponds to an isosceles trimer configuration.

$$\hat{V}_{\mathrm{dd}}(R_{mn}) = -\frac{\mu^2}{R_{mn}^3}|\pi_m\rangle\langle\pi_n|, \tag{2}$$

where $\mu = d_{\nu,1;\nu,0}/\sqrt{6}$ is the scaled radial matrix element. The nonresonant van der Waals interaction

$$\hat{V}_{\mathrm{VDW}}(R_{mn}) = -\frac{C_6}{2R_{mn}^6}\mathbb{I}, \tag{3}$$

ensures for $C_6 < 0$ repulsive behavior at very short distances regardless of the electronic state. Therefore, $\mathbb{I}$ denotes a unit matrix in the electronic space. We sketch, in [25], how this simple model of interactions arises from the full molecular physics of interacting Rydberg atoms using a magnetic field and selected total angular momentum states.

As previously shown [14–16,21], the joint motional and quantum state dynamics can be well understood from the eigenstates $|\varphi_k(\mathbf{R})\rangle$ of the electronic Hamiltonian $\hat{H}_{\mathrm{el}}(\mathbf{R}) = \sum_{m\neq n}[\hat{V}_{\mathrm{dd}} + \hat{V}_{\mathrm{VDW}}]$. These eigenstates and the corresponding eigenenergies $U_k(\mathbf{R})$ depend parametrically on $\mathbf{R}$ and are referred to as Frenkel excitons [1] and BO surfaces, respectively. The total wave function including atomic motion can be written as $|\Psi(\mathbf{R})\rangle = \sum_n \phi_n(\mathbf{R})|\varphi_n(\mathbf{R})\rangle$. To solve the coupled electronic and motional dynamics, we employ Tully's fewest switching algorithm [25,31–34], a quantum-classical method that is well established for our type of problem [15,16,35].

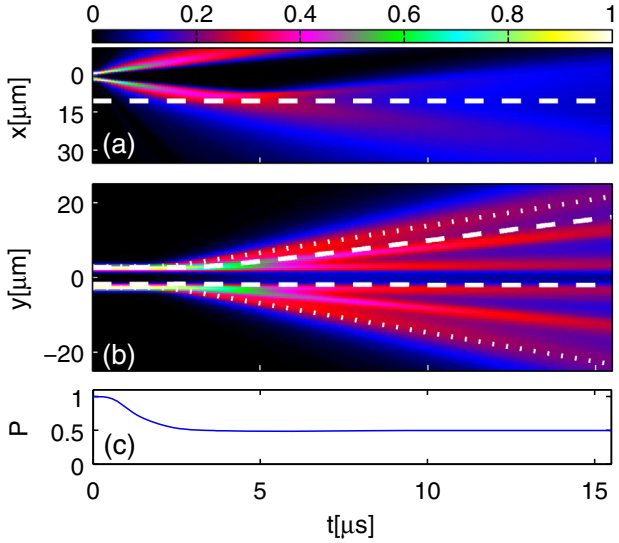

FIG. 2 (color online). Normalized total atomic density for atomic motion on two BO surfaces; overlayed are selected trajectories of the quantum classical method. (a) Horizontal density $n(x,t)$ (see [25]) of atoms 0 and 1. The dashed white line marks the x position of the vertical chain. (b) Vertical density $n(y,t)$ of atoms 2 and 3. In (a) and (b) we actually plot $\sqrt{n(x,t)}$, $\sqrt{n(y,t)}$. (c) Purity of reduced electronic state, see [25]. Our calculations are for lithium atoms excited to principal quantum number $\nu = 44$ with a transition dipole moment of $\mu = 1000$ a.u.. The parameters of the initial atomic configuration were $a_1 = 2.16$ μm, $a_2 = 5.25$ μm, and $d = 8.5$ μm. To sample the nuclear wave function, we have propagated 10^5 trajectories [36] with a standard deviation of $\sigma_x = 0.5$ μm for the atomic positions. Here, we have used $C_6 = 0$ for simplicity.

Two perpendicular dimers.—To realize a T shape chain, a minimum of two dimers is required, see Fig. 1(a). The atoms have a Gaussian distribution about their initial location $\mathbf{R}_0$ along their chain with width $\sigma = 0.5$ μm as sketched. Transverse to the chain, we assume perfect localization. The bars in Fig. 1(a) visualize the excitation amplitude of the exciton on the repulsive BO surface $|\varphi_{\mathrm{rep}}(\mathbf{R}_0)\rangle$. For each atom, the length of the bar shows $d_n = \langle\pi_n|\varphi_{\mathrm{rep}}(\mathbf{R}_0)\rangle$, orange for positive and blue for negative values. As one can see, initially the single p excitation in the system is shared among atoms 0 and 1. On the BO surface k, the force on atom n is given by $\mathbf{F}_{nk} = -\nabla_{\mathbf{R}_n} U_k(\mathbf{R})$. Because of the initial repulsive force $F_{\mathrm{n,rep}}$ (blue arrows) atom 1 moves and eventually reaches the position x_{CI}, where atoms 1–3 form a planar trimer. The two highest BO surfaces of this trimer conically intersect when the three atoms form an equilateral triangle, as shown in Fig. 1(b) and studied in detail in [21]. In the following, we will call these surfaces the repulsive (red) and middle (green) surface, respectively.

Exciton splitting.—Initialized on the repulsive surface of the global (double dimer) system, the exciton pulse is transferred to the vertical chain via the conical intersection onto these two electronic surfaces—the repulsive and the middle ones—dependent on the position of atom 1 relative to atoms 2 and 3 in the y direction when it enters the trimer configuration [see parameter p in Fig. 1(a)]. Viewed from the perspective of the trimer subsystem only, the exciton pulse enters on the middle surface, where the excitation amplitude (blue bar) matches the initial excitation distribution, see insets of Figs. 1(c) and 1(d). If atom 1 arrives right in the middle between atoms 2 and 3, the atomic trimer passes through the degenerate point of the CI leading to significant transfer of exciton amplitude to the repulsive surface [Fig. 1(c)]. If this is not the case, an asymmetric trimer configuration is realized for which nonadiabatic transitions, due to the CI, are much weaker, and the system remains on the middle trimer surface leading to the situation of Fig. 1(d) with quite different forces on atoms 2 and 3. This has profound consequences on the atomic motion: Amplitude on the repulsive surface leads to a symmetric repulsion of atoms 2 and 3 of the vertical chain, creating the outer pulses in the density shown in Fig. 2(b). A representative quantum-classical trajectory is shown as a white dotted line, with $p = 0.98$. On the repulsive surface, atom 1 is often reflected off the vertical chain as visible in Fig. 2(a). On the other hand, amplitude on the middle surface has the effect of a very asymmetric atomic motion in y, with that atom on the y axis remaining almost at rest, which has initially the smaller distance to the location of the dimer on the x axis. This type of motion is responsible for the inner and central features in Fig. 2(b), with a representative trajectory shown as white dashed lines with $p = 0.82$. One can also recognize the variant of the motion, where the other vertical atom remains at rest. The middle surface is mainly responsible for atom 1 freely passing the vertical chain in Fig. 2(a).

Since the nuclear wave packet of the exciton pulse will have a distribution of positions of atoms 1, 2, and 3, there will be in general a splitting of the exciton when it has passed the conical intersection with the electronic excitation propagating on the repulsive as well as the middle surface. In fact, about 50% of the initial amplitude has been transferred from the middle to the repulsive surface after 3 μs under the initial conditions for our exciton pulse leading to the dynamics of Fig. 2.

Hence, not only does the exciton split into two parts, traveling with the atoms in opposite directions in the y chain, we have a further coherent splitting of electronic excitation into the middle and repulsive electronic surface: The total initial wave function was $|\Psi_{\rm ini}(\mathbf{R})\rangle = \phi_0(\mathbf{R})|\varphi_{\rm rep}(\mathbf{R})\rangle$, where $\phi_0(\mathbf{R})$ describes the initial, harmonically trapped, spatial ground state. After the evolution shown in Fig. 2, the wave function reads $|\Psi_{\rm fin}(\mathbf{R})\rangle = \phi_{\rm rep}(\mathbf{R})|\varphi_{\rm rep}(\mathbf{R})\rangle + \phi_{\rm mid}(\mathbf{R})|\varphi_{\rm mid}(\mathbf{R})\rangle$.

In this final state $|\Psi_{\rm fin}(\mathbf{R})\rangle$, the atomic configuration and the electronic state are entangled, which can be quantified through the purity of the reduced electronic density matrix. It is obtained by averaging over the atomic position as described in [15,16,25]. The purity drops from one to $1/2$ when the exciton is split, as shown in Fig. 2(d), reflecting a transition from a pure to a mixed state. For the total (pure) system state, this implies a transition from a separable to an entangled state.

Exciton switch.—The minimal T shape system consisting of two dimers discussed so far primarily serves the purpose of elucidating the central element for exciton pulse control, namely, the junction between perpendicular atomic chains. Ultimately, we would like to interface the two dimers in Fig. 1(a) with longer atomic chains that can support exciton pulses as described in [15]. Such a pulse travels to the junction to become coherently split as just described, with the resulting exciton pulses on the vertical chain depending on how the conical intersection of the trimer at the junction was passed. Since the relative strength of the exciton pulse on the middle and repulsive surface of the trimer depends on the atomic positions and momenta near the conical intersection, we can control the exciton pulse propagation on the vertical chain, for example, via the position of the horizontal chain relative to the vertical one. We demonstrate this effect with three atoms on the horizontal and four atoms on the vertical chain, allowing for a vertical offset Δy of the horizontal chain from the center of the vertical chain, and a variable separation a_2 of the two central atoms in the second chain, see sketch in Fig. 4.

With small variations of the two parameters Δy, a_2, qualitatively very different scenarios can be realized, as illustrated with Fig. 3 and Fig. 4.

In scenario (a), the spacing a_2 and the shift Δy are so large that the trimer subunit discussed before does not form [37]. Since atom 2 approaches atom 4 closest (see Fig. 4), the exciton pulse travels in the downwards direction. To switch it upwards, we would use $\Delta y \to -\Delta y$. We characterize the relevant entanglement transport using $\bar{E}_{ij}$, the bipartite entanglement [15,16,25] during the last collision of the two terminal atoms i, j on the vertical chain, i.e., $(i, j) = (5, 6)$ upwards and $(i, j) = (3, 4)$ downwards. We know the last collision is in progress, whenever atom 3 (atom 6) reaches position $r_{\rm coll}$, indicated in Fig. 3 by horizontal white lines for the downwards (upwards) direction. Our results in Fig. 4 reveal that pulse propagation is linked with high fidelity entanglement transport, demonstrating successful control of the direction of exciton-pulse propagation without losing coherence.

In scenario (b), we segregate mechanical and electronic degrees of freedom of the exciton pulse, by choosing a_2 small enough such that a trimer subunit forms at the junction. Since an offset Δy is kept, the nuclear wave packet, however, misses the conical intersection and

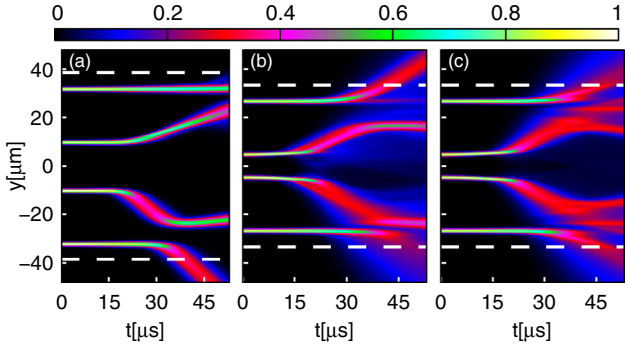

FIG. 3 (color online). Use of the trimer subunit with conical intersection as an exciton switch. Depending on the geometry, we can realize three qualitatively different scenarios: (a) asymmetric, repulsive surface; (b) asymmetric, middle surface; (c) symmetric, repulsive and middle surface. Each plot shows $\sqrt{n(y,t)}$ as in Fig. 2. When atoms reach the white horizontal lines (r_{coll}, 6.6 μm beyond the initial y position of atoms 3, 6), we extract the level of bipartite entanglement, listed in Fig. 4. The parameters, different from those of Fig. 2, are $\nu = 80$ (hence, $\mu = 3374$ a.u.), $a_1 = 6$ μm, $d = 22$ μm, and $C_6 \approx -7.6 \times 10^{20}$ a.u. as derived in [25]. Also, see [25] for videos of representative single trajectories.

remains on the middle trimer surface. Importantly, the middle trimer surface does not connect to a global surface allowing coherent exciton pulse transport: At the first collision within the vertical chain [between atoms 3 and 4 in Fig. 3(b)], part of the excitation evades those atoms and delocalizes on the remnant upper chain. Momentum is, henceforth, transported downwards by van der Waals collisions only such that the original exciton pulse with entangled atom and electron dynamics has been ripped apart. For this momentum transport without excitation transport, the inclusion of VDW interactions is crucial. They further cause the atom on the y axis closest to the x axis to carry most acceleration, in contrast to Fig. 2.

Finally, in scenario (c), $\Delta y = 0$ and the wave packet fully traverses the conical intersection at the junction. Here, the trimer subunit operates as described in the first part of the article. The wave packet is split onto both, the repulsive and middle trimer surfaces. As discussed for scenario (b), the middle trimer surface does not give rise to exciton-pulse propagation. On the repulsive surface, one gets symmetric (up-down) propagation of two pulses as expected. However, the entanglement transport in both directions is much weaker than in scenario (a), which is due to the fact that the atoms still share only a single p excitation. Subsequent nonadiabatic effects allow a strong coherent pulse only in a single direction. Even within this symmetric scenario, the relative importance of the middle and repulsive surfaces can be tuned via the effective size of the conical intersection [38], determined by atomic velocities and separation (energy splittings).

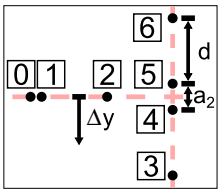

scenario	(a)	(b)	(c)
a_2	20μm	9.5μm	9.5μm
Δy	1.5μm	1.5μm	0
up, $\bar{E}_{56}$	0%	60%	24%
down, $\bar{E}_{34}$	97%	7%	24%

FIG. 4 (color online). Geometry and entanglement switching for the three scenarios of Fig. 3. Atom numbering and control parameters a_2, Δy are defined in the sketch on the left. The entanglement measure $\bar{E}_{ij}$ is defined in [25].

Conclusions.—We have shown how an exciton pulse can be coherently split through nonadiabatic dynamics at a conical intersection in a flexible Rydberg aggregate. Our results turn a junction between two Rydberg atom chains into a switch. The switch can control if and how exciton pulses continue to propagate in the system. Similar physics may be of interest for research on artificial light harvesting systems [39], where exciton transport and control is quintessential for energy efficiency. The atomic junction introduced here also provides a tool to directly examine the many-body dynamics near conical intersections in the laboratory.

The exciton splitting predicted could be experimentally monitored using high resolution Rydberg atom detection schemes [40–42], which are, in addition, state selective. Applied to our system, they allow a direct visualization of many-body wave packet dynamics near a conical intersection. The essential modular subunit of an atomic trimer exhibiting a CI can be envisaged as a building block for networks of exciton carrying atomic chains or a device for controlling the energy flow in molecular aggregates.

We gratefully acknowledge fruitful discussions with Alexander Eisfeld and Sebastian Möbius, as well as financial support by the Marie Curie Initial Training Network COHERENCE.

*karlo@pks.mpg.de

[1] J. Frenkel, Phys. Rev. **37**, 17 (1931).
[2] V. May and O. Kühn, *Charge and Energy Transfer Dynamics in Molecular Systems* (Wiley-VCH, Berlin, 2001).
[3] H. Park, P. J. Tanner, B. J. Claessens, E. S. Shuman, and T. F. Gallagher, Phys. Rev. A **84**, 022704 (2011).
[4] H. Park, E. S. Shuman, and T. F. Gallagher, Phys. Rev. A **84**, 052708 (2011).
[5] W. Li, P. J. Tanner, and T. F. Gallagher, Phys. Rev. Lett. **94**, 173001 (2005).
[6] S. Westermann, T. Amthor, A. de Oliveira, J. Deiglmayr, M. Reetz-Lamour, and M. Weidemüller, Eur. Phys. J. D **40**, 37 (2006).
[7] O. Mülken, A. Blumen, T. Amthor, C. Giese, M. Reetz-Lamour, and M. Weidemüller, Phys. Rev. Lett. **99**, 090601 (2007).

[8] S. Bettelli, D. Maxwell, T. Fernholz, C. S. Adams, I. Lesanovsky, and C. Ates, Phys. Rev. A **88**, 043436 (2013).
[9] G. Günter, H. Schempp, M. Robert-de-Saint-Vincent, V. Gavryusev, S. Helmrich, C. S. Hofmann, S. Whitlock, and M. Weidemüller, Science **342**, 954 (2013).
[10] S. Ravets, H. Labuhn, D. Barredo, L. Béguin, T. Lahaye, and A. Browaeys, arXiv:1405.7804.
[11] D. Barredo, H. Labuhn, S. Ravets, T. Lahaye, A. Browaeys, and C. S. Adams, arXiv:1408.1055.
[12] T. F. Gallagher, *Rydberg Atoms* (Cambridge University Press, Cambridge, England, 1994).
[13] I. I. Beterov, D. B. Tretyakov, I. I. Ryabtsev, V. M. Entin, A. Ekers, and N. N. Bezuglov, New J. Phys. **11**, 013052 (2009).
[14] C. Ates, A. Eisfeld, and J. M. Rost, New J. Phys. **10**, 045030 (2008).
[15] S. Wüster, C. Ates, A. Eisfeld, and J. M. Rost, Phys. Rev. Lett. **105**, 053004 (2010).
[16] S. Möbius, S. Wüster, C. Ates, A. Eisfeld, and J. M. Rost, J. Phys. B **44**, 184011 (2011).
[17] A. Asadian, M. Tiersch, G. G. Guerreschi, J. Cai, S. Popescu, and H. J. Briegel, New J. Phys. **12**, 075019 (2010).
[18] A. Eisfeld, Chem. Phys. **379**, 33 (2011).
[19] S. K. Saikin, A. Eisfeld, S. Valleau, and A. Aspuru-Guzik, Nanophotonics **2**, 21 (2013).
[20] O. Kühn and S. Lochbrunner, Semicond. Semimet. **85**, 47 (2011).
[21] S. Wüster, A. Eisfeld, and J. M. Rost, Phys. Rev. Lett. **106**, 153002 (2011).
[22] W. Domcke, D. R. Yarkony, and H. Köppel, *Conical Intersections* (World Scientific, Singapore, 2004).
[23] L. Li, Y. O. Dudin, and A. Kuzmich, Nature (London) **498**, 466 (2013).
[24] R. Mukherjee, J. Millen, R. Nath, M. P. A. Jones, and T. Pohl, J. Phys. B **44**, 184010 (2011).
[25] See Supplemental Material at http://link.aps.org/supplemental/10.1103/PhysRevLett.113.223001 for additional details regarding the employed quantum-classical algorithm, the Rydberg trimer subunit, our purity and entanglement measure, extraction of total atomic densities and the realization of isotropic dipole-dipole interactions, which includes Refs. [26–30].
[26] T. Carrington, Acc. Chem. Res. **7**, 20 (1974).
[27] C. A. Mead and D. G. Truhlar, J. Chem. Phys. **70**, 2284 (1979).
[28] S. Hill and W. K. Wootters, Phys. Rev. Lett. **78**, 5022 (1997).
[29] W. K. Wootters, Phys. Rev. Lett. **80**, 2245 (1998).
[30] P. Goy, J. Liang, M. Gross, and S. Haroche, Phys. Rev. A **34**, 2889 (1986).
[31] J. C. Tully and R. K. Preston, J. Chem. Phys. **55**, 562 (1971).
[32] S. Hammes-Schiffer and J. C. Tully, J. Chem. Phys. **101**, 4657 (1994).
[33] M. Barbatti, Wiley Interdiscip. Rev.: Comput. Mol. Sci. **1**, 620 (2011).
[34] A. Jasper and D. Truhlar, J. Chem. Phys. **122**, 044101 (2005).
[35] S. Möbius, M. Genkin, A. Eisfeld, S. Wuster, and J. M. Rost, Phys. Rev. A **87**, 051602 (2013).
[36] G. R. Dennis, J. J. Hope, and M. T. Johnsson, Comput. Phys. Commun. **184**, 201 (2013).
[37] Considering a trimer subunit only makes sense in a moment where three atoms have clearly closer mutual separations than all others.
[38] E. Teller, J. Phys. Chem. **41**, 109 (1937).
[39] I. McConnell, G. Li, and G. W. Brudvig, Chem. Biol. **17**, 434 (2010).
[40] A. Schwarzkopf, R. E. Sapiro, and G. Raithel, Phys. Rev. Lett. **107**, 103001 (2011).
[41] B. Olmos, W. Li, S. Hofferberth, and I. Lesanovsky, Phys. Rev. A **84**, 041607(R) (2011).
[42] G. Günter, M. Robert-de-Saint-Vincent, H. Schempp, C. S. Hofmann, S. Whitlock, and M. Weidemüller, Phys. Rev. Lett. **108**, 013002 (2012).